Published in final edited form as:
J Org Chem. 2009 August 21; 74(16): 5902–5908. doi:10.1021/jo900844r.

Fibrosterol Sulfates from the Philippine Sponge *Lissodendoryx* (*Acanthodoryx) fibrosa*; Sterol Dimers that Inhibit PKCζ

Emily L. Whitson[†], **Tim S. Bugni**[†], **Priya S. Chockalingam**[‡], **Gisela P. Concepcion**[§], **Xidong Feng**[‡], **Guixian Jin**[‡], **Mary Kay Harper**[†], **Gina C. Mangalindan**[§], **Leonard A. McDonald**[‡], and **Chris M. Ireland**[†,*]

[†]Department of Medicinal Chemistry, University of Utah, Salt Lake City, Utah 84112

[‡]Wyeth Research, Pearl River, New York 10965

[§]Marine Science Institute, University of the Philippines, Diliman 1101, Quezon City, Philippines

Introduction

Polyoxygenated[1] and polysulfated steroids with atypical, modified side chains,[2] are prevalent among compounds isolated from marine organisms. Sponge-derived sulfated sterols have a wide array of reported biological activities in a variety of therapeutic areas. Of particular note is their activity against HIV-1.[3–5] In addition, the spheciosterol sulfates A–C, isolated from a *Spheciospongia* sp. sponge, were recently shown to inhibit protein kinase C ζ (PKCζ), as well as downstream NF-κB activation.[6] PKCζ has been implicated as an integral factor in several types of cancer,[7–11] obesity,[12] and osteoarthritis.[8,13] Consequently, the detection and identification of PKCζ-specific inhibitors could have a potentially profound impact on the treatment of a number of diseases and disorders.

As part of an ongoing search for bioactive marine metabolites, crude extracts from our marine invertebrate library were screened for PKCζ inhibition. The methanol extract of a *Lissodendoryx* (*Acanthodoryx*) *fibrosa* sample, collected from Coron Island, Philippines, showed promising PKCζ inhibition in the initial screening. No natural products had been reported from this sponge, suggesting *L. (A.) fibrosa* would be an attractive source for chemical investigation. As a result, fibrosterol sulfates A–C (**1**–**3**), three new sulfated bis-steroids, were isolated from the sponge. Data from several experiments verified that fibrosterol sulfates A (**1**) and B (**2**) were, in fact, PKCζ inhibitors.

[*]To whom correspondence should be addressed. Tel: (801) 581-8305. Fax: (801) 585-6208. cireland@pharm.utah.edu.

Supporting Information Available: ^{1}H spectra of **1**–**3**, ^{13}C spectra of **1** and **2**, HSQC spectrum of **3**, methods attempted to determine the configuration of C-22 and the cyclopentane ring in **1**, a table of interatomic distances for **3** from molecular modeling, and a simplified 3D representation of **3**. This material is available free of charge via the Internet at http://pubs.acs.org.

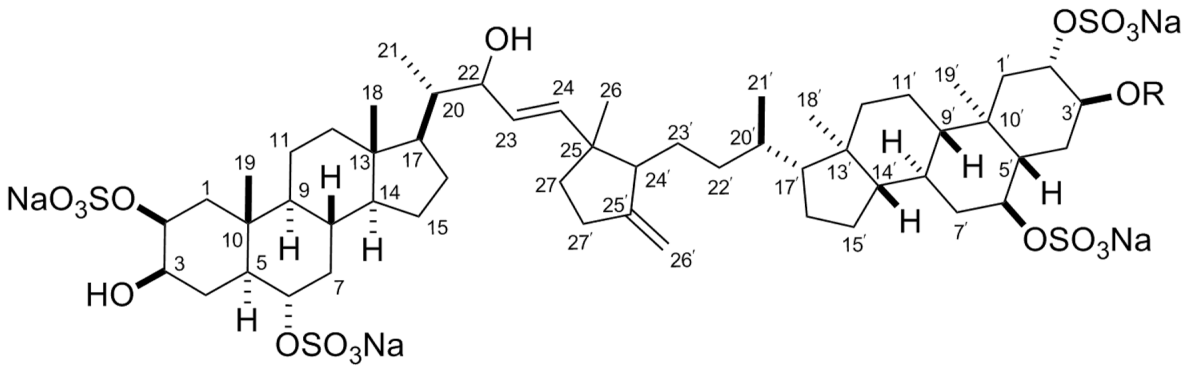

1 R = H

2 R = SO_3Na

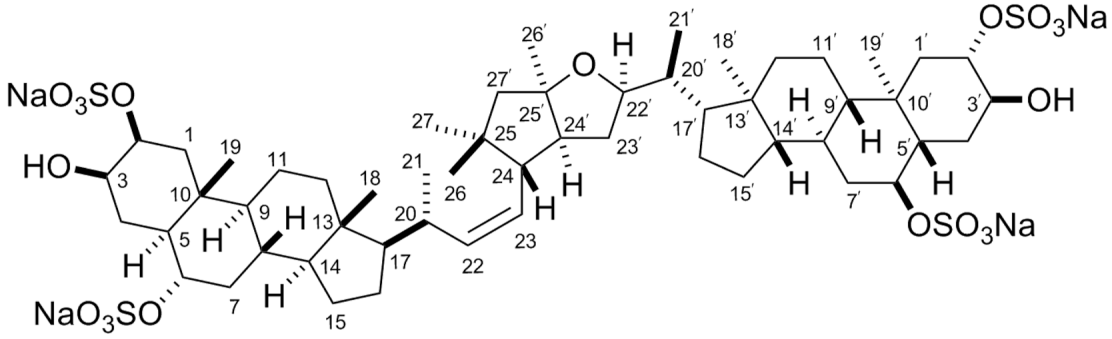

3

Results and Discussion

The *L.* (*A.) fibrosa* specimen (PC00-04-56) was exhaustively extracted with MeOH and the crude extract separated on an HP20SS resin using a step gradient of H_2O to isopropanol (IPA) (25% steps, 5 fractions). Bioassay-guided fractionation of the second (75/25 H_2O/IPA) and third fractions (50/50 H_2O/IPA), utilizing reversed-phase column chromatography and reversed-phase HPLC, resulted in the isolation of fibrosterol sulfates A–C (**1**–**3**).

The molecular formula for fibrosterol sulfate A (**1**), $C_{54}H_{84}O_{19}S_4Na_4$, was derived from NMR data and the HRESIMS ion at *m/z* 605.2147 ($[M-2Na]^{-2}$; Δ +0.21 ppm). Utilizing the ultra-high resolution capabilities of FTMS, the ^{34}S peak could be resolved from the $^{13}C_2$ peak, indicating the presence of four sulfurs in **1**. The presence of multiply charged ions in the mass spectra coupled with characteristic sulfate losses in FT-MS/MS experiments indicated that sulfate esters were present in **1**. The structure of fibrosterol sulfate A (**1**) was established on the basis of extensive 1D and 2D NMR studies. Initial interpretation of the NMR data (Table 1) suggested that **1** was an isoprenoid containing five methyl singlets (δ_H 0.71, 0.72, 1.05, 1.08, 1.15), two methyl doublets (δ_H 0.97, 0.99), seven oxygenated methines (δ_H 3.58, 3.98, 4.06, 4.19 (2), 4.46, 4.64), a *trans* olefin (δ_H 5.35, *J* = 15.7; 5.54, *J* = 15.7) and a terminal olefin (δ_H 4.85, 4.81). The data also indicated that fibrosterol sulfate A (**1**) contained six quaternary

carbons, 22 methines, and 19 methylenes. Many of the signals, specifically the methyls, appeared in pairs, indicating that **1** was a pseudo-symmetrical bis-steroid. The pseudo-symmetrical nature of the molecule created an overlap of spectral resonances which complicated data interpretation at lower field strength (500 MHz). However, the increased sensitivity and resolution, afforded by a 600 MHz instrument equipped with a cryoprobe, allowed for clear interpretation of the overlapping signals in **1**. Analysis of COSY and HMBC data led to the assignment of the ABCD and A′B′C′D′ steroid ring systems in fibrosterol sulfate A (**1**) (Table 1). Rings A and B were assembled based on COSY correlations among all adjacent protons between H-1 and H-9. HMBC correlations from Me-19 to C-1, C-5, C-9 and C-10 completed the structural assignment of the A and B rings. Rings C and D were assigned based on HMBC correlations from Me-18 to C-12, C-13, C-14 and C-17; and H-14 to C-8, C-13, and C-15. COSY correlations between H-11 and H-9, and H-11 and H-12; and HMBC correlations from H-11 to C-9 and C-12 supported the connectivity of C-9 through C-12. HMBC correlations from H-16 to C-17 and C-15 completed the structural assignment of the C and D rings. The A′B′C′D′ rings were assembled in the same fashion; all of the correlations used to assign the ABCD rings were identical to the correlations used to assign the A′B′C′D′ rings. HMBC correlations from Me-21, Me-26 and Me-21′ were particularly useful in constructing the side chain that fuses rings D and D′ in **1** (HMBC correlations from Me-21 to C-17, C-20 and C-22; Me-21′ to C17′, C-20′ and C-22′; Me-26 to C-24, C-25, C-27 and C-24′). COSY correlations between H-22 and H-23, and H-23 and H-24, in addition to the methyl correlations, supported all connectivities between C-20 and C-27. HMBC correlations from H-23′ to C-22′ and C-24′; and H-26′ to C-24′ and C-27′, supported all connectivities between C-20′ and C-27′. COSY correlations between H-27 and H-27′, as well as HMBC correlations from H-27′ to C-27, completed the assignment of the side chain that joins the two steroid units in fibrosterol sulfate A (**1**). Sulfates induce a downfield ^{13}C shift of ~5–9 ppm on the δ_C of C-2, C-3 and C-6 when compared to the corresponding triols.[14–16] As such, the sulfate groups were assigned to C-2, C-6, C-2′, and C-6′, and hydroxyls were placed at C-3, C-3′, and C-22 in fibrosterol sulfate A (**1**).

Because of a significant number of overlapping ^{1}H signals, few coupling constants could be obtained for fibrosterol sulfate A (**1**), complicating the relative configuration analysis. However, biosynthetic precedents and ROESY data clearly indicated that **1** contained two standard 5α10β steroid nuclei (Figure 1). ROESY data, w-coupling, and ^{13}C chemical shift analysis were all necessary to determine the configuration at C-2, C-3, C-6, C-2′, C-3′, and C-6′. H-2 was given an equatorial assignment based on the observed w-coupling between H-2 and H-4α in the COSY spectrum, and the narrow multiplicities for H-2 in the ^{1}H spectrum (absence of large vicinal coupling constants). H-3 was designated axial based on the presence of a large vicinal coupling constant (J = 11.8 Hz) and the ROE observed between H-3 and H-5. H-6 was given an axial assignment based on the ROE observed between H-6 and Me-19. The ^{13}C chemical shifts in the AB rings were compared with AB steroid rings containing different configurations at C-2, C-3, and C-6.[16–21] The configuration of the AB rings in fibrosterol sulfate A (**1**) corresponded best to that observed in amaranzole A,[19] as 2*S*, 3*R*, 6*S*. Chemical shift variances observed between the AB and A′B′ rings suggested configuration differences, which were confirmed after careful observation of several parameters. The narrow multiplicities for H-2′ and H-3′ in the ^{1}H spectrum and the lack of a ROE between H-2′ and Me-19′, and H-3′ and H-5′ implied that H-2′ and H-3′ were equatorial. It is probable that w-coupling between H-2′ and H4 α′ and H-3′ and H1β′ occurs; however, the signal overlap of H4α′ and H1β′ (δ_H 2.04 and 2.06, respectively) precludes discrete observation in the COSY spectrum. H-6′ was given an axial assignment based on the ROE observed between H-6′ and Me-19′. ^{13}C chemical shifts in the A′B′ rings were compared with AB steroid rings containing different configurations at C-2, C-3, and C-6.[16–21] The configuration of the A′B′ rings in fibrosterol sulfate A (**1**) was consistent with the configurations of halistanol sulfate[16] and a semi-synthetic sterol,[22] as 2′*S*, 3′*S*, 6′*S*. *J*-based analysis of **1** was used in an attempt to assign

the relative configuration of the C-22 alcohol,[23] but the results were inconclusive (see Supporting Information). Molecular modeling studies were conducted on four diastereomers of **1** (25*R*,24′*S*; 25*S*,24′*R*; 25*R*,24′*R*; and *25S,24′S*), and interatomic distances were calculated (Supplemental Table 1) in an effort to determine if ROEs could be used to distinguish whether the ring in **1** had a *cis* or *trans* relative configuration. However, no conclusive results could be obtained (see Supporting Information). Ongoing studies using RDC analysis should aid in the assignment of the C-22 configuration as well as the configuration at C-25 and C-24′. Based on the aforementioned data, fibrosterol sulfate A (**1**) was assigned as 2*S*, 3*R*, 5*S*, 6*S*, 8*S*, 9*S*, 10*R*, 13*S*, 14*S*, 17*R*, 20*R*, 23*E*, 2′*S*, 3′*S*, 5′*S*, 6′*S*, 8′*S*, 9′*S*, 10′*R*, 13′*S*, 14′*S*, 17′*R*, 20′*R*.

The molecular formula for fibrosterol sulfate B (**2**), $C_{54}H_{83}O_{22}S_5Na_5$, was derived from NMR data and the HRESIMS ion at *m/z* 656.1843 ([M-2Na]$^{-2}$, Δ−0.35 ppm). FT-MS analysis indicated five sulfur atoms were present in the molecular formula for **2**. Characteristic sulfate losses in FT-MS/MS experiments combined with multiply charged ions in the mass spectra indicated that **2** also contained sulfate esters. Comparison of the molecular formulas for **1** and **2** revealed that fibrosterol sulfate B (**2**) contained an additional sulfate group. The NMR spectra of fibrosterol sulfates A (**1**) and B (**2**) are very similar, with the major ^{1}H and ^{13}C chemical shift differentials between the two molecules occurring in the A′ ring (Table 1 and Table 2). All of the data suggested that the only difference between the two molecules was an additional sulfate in **2** at C-3′.

The molecular formula for the minor compound fibrosterol sulfate C (**3**), $C_{54}H_{84}O_{19}S_4Na_4$, was derived from NMR data and the HRESIMS ion at *m/z* 1233.4167 ([M-Na]$^-$, Δ−1.3 ppm). Compound **3** showed a similar ^{1}H NMR spectrum and identical molecular formula when compared with **1**, which suggested that **3** was also a sulfated bis-steroid. Comparison of the NMR data for fibrosterol sulfates A (**1**) and C (**3**) indicated that the ABCD and A′B′C′D′ rings are virtually indistinguishable, while the side chains are quite different (Table 1 and Table 3). The side chain of fibrosterol sulfate C (**3**) lacked the terminal olefin seen in **1**, but contained a *cis* olefin (δ_H 5.29, J = 10.8; 5.02, J = 10.8), three singlet methyls, an oxygenated methine (δ_C 82.4; δ_H 4.16) and a deshielded quaternary carbon (δ_C 91.0). HMBC correlations from Me-21, Me-26, Me-27, Me-21′, and Me-26′ were essential for constructing the side chain that fuses rings D and D′ in **3**. HMBC correlations from Me-21 to C-17, C-20 and C-22, Me-26 to C-24, C-25, C-27 and C-27′, Me-27 to C-24, C-25, C-26 and C-27′, and COSY correlations between H-22 and H-23, and H-23 and H-24, supported all connectivities between C-20 and C-27. HMBC correlations from Me-21′ to C-17′, C-20′ and C-22′, Me-26′ to C-24′, C-25′ and C-27′, and COSY correlations between H-22′ and H-23a/b′, and H-23a/b′and H-24′, supported all connectivities between C-20′ and C-27′. HMBC correlations from Me-26 and Me-27 suggested that C-25 and C-27′ were connected, which was further supported by HMBC correlations between H-27a/b′ and C-25, C-26, C-27, C-25′, C-26′. COSY correlations between H-24 and H-24′ and HMBC correlations from H-24 to C-24′, and H-24′ to C-24 supported a connection between C-24 and C-24′ to form the cyclopentane ring in **3**. The molecular formula for fibrosterol sulfate C (**3**) required 11 degrees of unsaturation, suggesting that the final degree of unsaturation was an ether linkage between C-22′ and C-25′to give the oxabicyl[3,3,0]octane seen in **3**. The unusual quaternary ether carbon ^{13}C chemical shift (δ_C 91.0, C-25′) was compared to similar ring systems seen in ibhayinol (δ_C 91.4),[24] and kuhistaferone (δ_C 100.4),[25] and was consistent with the oxabicyl[3,3,0]octane for **3** as drawn.

Fibrosterol sulfate C (**3**) exhibited identical ROESY data to **1** for the ABCD and A′B′C′D′ rings, supporting a 2*S*, 3*R*, 6*S*, 2′*S*, 3′*S*, 6′*S* configuration for **3**. ROESY data and molecular modeling were utilized to determine the relative configuration of the oxabicyl[3,3,0]octane in **3** (Figure 2 and Supporting Information). ROEs between Me-26′and H-24′supported a *cis* ring juncture, with both Me-26′ and H-24′ being in the α configuration. ROEs between Me-26′ and H-22′ indicated that H-22′ was also in the α configuration. ROEs between H-24′ and Me-27

established that Me-27 was in the α configuration, while ROEs between Me-26 and H-24 suggested that H-24 was in the β configuration. The large coupling constant observed between H-24 and H-24′ (J = 10.1 Hz) also supported a *trans* relationship between H-24 and H-24′. Based on these data, fibrosterol sulfate C (**3**) was assigned as 2*S*, 3*R*, 5*S*, 6*S*, 8*S*, 9*S*, 10*R*, 13*S*, 14*S*, 17*R*, 20*R*, 22*Z*, 24*S**, 2′*S*, 3′*S*, 5′*S*, 6′*S*, 8′*S*, 9′*S*, 10′*R*, 13′*S*, 14′*S*, 17′*R*, 20′*R*, 22′*R**, 24′*S**, 25′*R**. The relative configuration between C-24 and C-22′ could not be relayed through C-20′ due to overlapping signals; H-20′ and H-23β′ chemical shifts are identical (δ_H1.84), as well as H-21′ and H-17′(δ_H 1.00).

Fibrosterol sulfates A (**1**) and B (**2**) inhibited PKCζ with IC_{50} values of 16.4, and 5.6 μM, respectively. Fibrosterol sulfate C (**3**) was not tested for biological activity due to the limited amount of material isolated. The risk of a false-positive was eliminated by employing a counter screen that ensured **1** and **2** were not interfering with the signal detection. Compounds **1** and **2** were incubated with the phosphorylated U*Light*™-PKC peptide and the antibody, and the TR-FRET signals were measured at 665 nm. The TR-FRET signals remained constant when **1** and **2** were incubated with the phosphorylated U*Light*™-PKC peptide and the antibody, thereby eliminating the possibility of false-positive inhibition by this mechanism. Light scattering measurements also indicated that fibrosterol sulfates A (**1**) and B (**2**) were soluble at PKCζ assay concentrations, ruling out the possibility that **1** and **2** were false positives due to aggregate formation.

The spheciosterol sulfates A-C, isolated from a *Spheciospongia* sp., were recently shown to inhibit PKCζ and NF-κB activation.[6] It was shown that the sterol side chain factors into their PKCζ activity; the longer side chain seen in spheciosterol sulfate C is 5-fold more active than spheciosterol sulfate B, and 10-fold more active than the shorter side chains seen in spheciosterol sulfate A and topsentiasterol sulfate E.[6] The number of sulfates also appears to be important for PKCζ activity, as fibrosterol sulfate B (**2**) is 3-fold more active than fibrosterol sulfate A (**1**). Interestingly, the spheciosterol sulfates and the fibrosterol sulfates share a similar oxygenation pattern in the steroid rings, suggesting that the steroid oxygenation pattern may also be important for PKCζ inhibition.

Fibrosterol sulfates A–C (**1**–**3**) appear to be composed of two cholestene monomers, with differing configuration at C-3, and oxygenation at C-22 in only one monomer. These molecules would be excellent candidates for future biosynthetic studies.

Previous investigations of sponges from the genus *Lissodendoryx* have yielded steroids,[26,27] pyrrololactams,[28] cembranes,[29] and polyether macrolides.[30,31] Only a few steroid dimers have been isolated from marine organisms such as cephalostatins,[32–39] crellastatins,[40–42] ritterazines,[43–46] hamigerols,[47] bistheonellasterone,[48] and amaroxocanes.[49] The cephalostatins,[32–39] ritterazines[43–46] and bistheonellasterone[48] are all fused between the A and A′ rings, while the crellastains,[40–42] hamigerols,[48] and amaroxocane B[49] are fused through the side chains to form a dioxabicyclononane ring system. Amaroxocane A[49] and crellastatin M[42] contain a carbacylic ring fusion similar to the cyclopentane seen in fibrosterol sulfates A and B. Fibrosterol sulfate C (**3**) is unique in that there has never been a report of the oxabicyclo [3,3,0] octane in a dimeric sterol.

Experimental Section

Biological Material

L. (*A*.) *fibrosa* (Lévi, 1961) (Coelosphaeridae), sample PC00-04-56, was collected by SCUBA from Coron Island (11° 57.833′N, 120° 06.311′E), northern Palawan, Philippines; a voucher specimen is maintained at the University of Utah.

Extraction and Isolation

The *Lissodendoryx* (*Acanthodoryx*) *fibrosa* specimen (PC00-04-56) was exhaustively extracted with MeOH to yield 2.60 g of crude extract. The crude extract was separated on HP20SS resin using a step gradient of H_2O to IPA in 25% steps, and a final wash of 100% MeOH, to yield 5 fractions. The second fraction (0.46 g; 75/25 H_2O/IPA) was chromatographed on C_{18} (32 × 10 cm) using a step gradient of 100% 0.2 M aq. NaCl to CH_3CN in 10% steps, and a final wash of 100% MeOH, to yield 12 fractions (175A – 175L). The third HP20SS fraction (50/50 H_2O/IPA) was also chromatographed on C_{18} (32 × 10 cm) using the same gradient, to yield 12 fractions (185A – 185L). Fractions 175D (20.4 mg; 30% CH_3CN/70% 0.2 M NaCl in H_2O), 175E (7.2 mg; 40% CH_3CN/60% 0.2 M NaCl in H_2O), 185E (27.4 mg; 40% CH_3CN/60% 0.2 M NaCl in H_2O) and 185F (15.4 mg; 50% CH_3CN/50% 0.2 M NaCl in H_2O) were combined. The combined fractions were purified by HPLC using a C_{18} column (250 × 10 mm) employing a gradient of 2% CH_3CN/98% 0.2 M NaCl in H_2O to 30% CH_3CN/70% 0.2 M NaCl in H_2O over 5 min, followed by a gradient of 30% CH_3CN/70% 0.2 M NaCl in H_2O to 50% CH_3CN/50% 0.2 M NaCl in H_2O at 4.5 mL/min over 32 minutes to yield fibrosterol sulfate A (**1**, 6.4 mg) eluting at 18.6 min and fibrosterol sulfate B (**2**, 8.0 mg) eluting at 16.1 min.

An aliquot of the third HP20SS fraction (186 mg; 50/50 H_2O/IPA) was chromatographed on LH20 (24 × 2.5 cm) using MeOH as eluant, to yield 67 fractions (138.1–138.67). Fraction 138.4 was purified by HPLC using a C_8 column employing a gradient of 10% CH_3CN/H_2O to 35% CH_3CN/H_2O at 4 mL/min over 33 minutes to yield 9 fractions (159A–159I). Fraction 159I was further purified by HPLC using a C_{18} column (250 × 10 mm) employing a gradient of 2% CH_3CN/98% 0.2 M NaCl in H_2O to 30% CH_3CN/70% 0.2 M NaCl in H_2O over 5 min, followed by a gradient of 30% CH_3CN/70% 0.2 M NaCl in H_2O to 50% CH_3CN/50% 0.2 M NaCl in H_2O at 4.5 mL/min over 32 minutes to yield fibrosterol sulfate C (**3**, 0.3 mg) eluting at 28.4 minutes.

Desalting of the flash column and HPLC fractions was achieved by filtering the samples through C_{18} Sep-Pak cartridges; salts were removed by washing with 100% H_2O, and individual fractions or compounds were eluted with 100% MeOH.

Fibrosterol Sulfate A (1)

Amorphous white solid, $[\alpha]^{22}_{D}$ +16.2 (*c* 0.08, MeOH); UV (MeOH) λ_{max} (log ε) 206 (3.70) nm; IR (film, NaCl) ν_{max} 3377 (br), 1660, 1641, 1444, 1221, 1063, 966, 708 cm^{-1}; ^1H NMR and ^{13}C NMR data, see Table 1; HRESIMS *m/z* 605.1459 $[M-2Na]^{-2}$ (calcd for $C_{54}H_{84}O_{19}S_4Na_2$, 605.1480).

Fibrosterol Sulfate B (2)

Amorphous white solid, $[\alpha]^{22}_{D}$ +19.1 (*c* 0.10, MeOH); UV (MeOH) λ_{max} (log ε) 206 (3.91) nm; IR (film, NaCl) ν_{max} 3224 (br), 1662, 1639, 1444, 1221, 968, 714 cm^{-1}; ^1H NMR and ^{13}C NMR data, see Table 2; HRESIMS *m/z* 656.18432 $[M-2Na]^{-2}$ (calcd for $C_{54}H_{83}O_{22}S_5Na_3$, 656.18418).

Fibrosterol Sulfate C (3)

Amorphous white solid,$[\alpha]^{20}_{D}$ +29.2 (*c* 0.13, MeOH); UV (MeOH) λ_{max} (log ε) 204 (4.04) nm; IR (film, NaCl) ν_{max} 3346 (br), 2953, 1662, 1641, 1446, 1219, 1063, 962, 708 cm^{-1}; ^1H NMR and ^{13}C NMR data, see Table 3; HRESIMS *m/z* 1233.4167 $[M-Na]^-$(calcd for $C_{54}H_{84}O_{19}S_4Na_3$, 1233.4183).

PKCζ assay

IC_{50} values were determined in a homogenous TR-FRET based PKCζ kinase activity assay (LANCE-Ultra, Perkin Elmer). Compounds **1** and **2**, at various concentrations, were incubated with the U*Light*™-PKC peptide substrate (50 nM), ATP (2 μM), and PKCζ (25 pM). The reaction was stopped with EDTA (15 mM) after 60 min, Eu-labeled anti-phospho-PKC peptide antibody was added, and the extent of phospho-peptide product formation was determined through the measurement of the TR-FRET signals at 615 nm and 665 nm wavelengths upon excitation at 340 nm. A decrease in the TR-FRET signal ratio was observed as a function of increasing compound concentration and the IC_{50} for each compound was determined accordingly.

Supplementary Material

Refer to Web version on PubMed Central for supplementary material.

Acknowledgments

The authors would like to thank Dr. M. He, Dr. F. Ritacco, Y. Zhang, Dr. G. Schlingmann, Dr. F. E. Koehn, and Dr. G.T. Carter, Wyeth Research, for their kind support. We acknowledge the NIH, Grants RR13030, RR06262, and NSF Grant DBI-0002806 for funding NMR instrumentation in the University of Utah Health Sciences NMR Facility. This research was supported by NCI grant CA67786 and NIH grant CA36622 (C.M.I.).

References and Notes

1. Sarma NS, Krishna MSR, Rao SR. Mar. Drugs 2005;3:84–111.
2. D'Auria MV, Minale L, Riccio R. Chem. Rev 1993;93:1839–1895.
3. McKee TC, Cardellina JH II, Riccio R, D'Auria MV, Iorizzi M, Minale L, Moran RA, Gulakowski RJ, McMahon JB, Buckheit RW Jr, Snader KM, Boyd MR. J. Med. Chem 1994;37:793–797. [PubMed: 8145229]
4. Lerch ML, Faulkner DJ. Tetrahedron 2001;57:4091–4094.
5. Sun HH, Cross SS, Gunasekera M, Koehn FE. Tetrahedron 1991;47:1185–1190.
6. Whitson EL, Bugni TS, Chockalingam PS, Concepcion GP, Harper MK, He M, Hooper JN, Mangalindan GC, Ritacco F, Ireland CM. J. Nat. Prod 2008;71:1213–1217. [PubMed: 18558742]
7. Guo H, Ma Y, Zhang B, Sun B, Niu R, Ying G, Zhang N. J. Leukoc. Biol. 2009
8. Zhao C, Cai M, Zhang Y, Liu Y, Sun R, Zhang N. Anal. Biochem 2007;362:8–15. [PubMed: 17240347]
9. Cohen EEW, Lingen MW, Zhu B, Zhu H, Straza MW, Pierce C, Martin LE, Rosner MR. Cancer Res 2006;66:6296–6303. [PubMed: 16778206]
10. Sun R, Gao P, Chen L, Ma D, Wang J, Oppenheim JJ, Zhang N. Cancer Res 2005;65:1433–1441. [PubMed: 15735031]
11. Mustafi R, Cerda S, Chumsangsri A, Fichera A, Bissonnette M. Mol. Cancer. Res 2006;4:683–694. [PubMed: 16940160]
12. Sajan MP, Standaert ML, Nimal S, Varanasi U, Pastoor T, Mastorides S, Braun U, Leitges M, Farese R. J. Lipid. Res. 2009
13. LaVallie ER, Chockalingam PS, Collins-Racie LA, Freeman BA, Keohan CC, Leitges M, Dorner AJ, Morris EA, Majumdar MK, Arai M. J. Biol. Chem 2006;281:24124–24137. [PubMed: 16798739]
14. Gunasekera SP, Sennett SH, Kelly-Borges M, Bryant RW. J. Nat. Prod 1994;57:1751–1754. [PubMed: 7714543]
15. Umeyama A, Adachi K, Ito S, Arihara S. J. Nat. Prod 2000;63:1175–1177. [PubMed: 10978223]
16. Fusetani N, Matsunaga S, Konosu S. Tetrahedron Lett 1981;22:1985–1988.
17. Ramirez JA, Brosa C, Galagovsky LR. Phytochem 2005;66:581–587.
18. Carotenuto A, Fattorusso E, Lanzotti V, Magno S, De Feo V, Carnuccio R, D'Acquisto F. J. Nat. Prod 1997;60:1003–1007. [PubMed: 9358643]

19. Morinaka BI, Masuno MN, Pawlik JR, Molinski TF. Org Lett 2007;9:5219–5222. [PubMed: 17990891]
20. Mimaki Y, Kuroda M, Fukasawa T, Sashida Y. J. Nat. Prod 1999;62:194–197. [PubMed: 9917320]
21. Mimaki Y, Sashida Y. Chem. Pharm. Bull 1990;38:1090–1092.
22. Makarieva TN, Gorshkova IA, Gorshkov BA, Kalinovskii AI, Stonik VA. Khim. Prir. Soedin 1986;4:441–445.
23. Matsumori N, Kaneno D, Murata M, Nakamura H, Tachibana K. J. Org. Chem 1999;64:866–876. [PubMed: 11674159]
24. McPhail KL, Davies-Coleman MT, Copley RCB, Eggleston DS. J. Nat. Prod 1999;62:1618–1623.
25. Tamemoto K, Takaishi Y, Kawazoe K, Honda G, Ito M, Kiuchi F, Takeda Y, Kodzhimatov OK, Ashurmetov O, Shimizu K, Nagasawa H, Uto Y, Hori H. J. Nat. Prod 2002;65:1323–1324. [PubMed: 12350156]
26. Sheikh YM, Djerassi C. Tetrahedron 1974;30:4095–4103.
27. Silva CJ, Djerassi C. Collect. Czech. Chem. Commun 1991;56:1093–1105.
28. Schmitz FJ, Gunasekera SP, Lakshmi V, Tillekeratne LMV. J. Nat. Prod 1985;48:47–53. [PubMed: 2861253]
29. Fontana A, Ciavatta ML, Amodeo P, Cimino G. Tetrahedron 1999;55:1143–1152.
30. Litaudon M, Hart JB, Blunt JW, Lake RJ, Munro MHG. Tetrahedron Lett 1994;35:9435–9438.
31. Litaudon M, Hickford SJH, Lill RE, Lake RJ, Blunt JW, Munro MHG. J. Org. Chem 1997;62:1868–1871.
32. Pettit GR, Inoue M, Kamano Y, Herald DL, Arm C, Dufresne C, Christie ND, Schmidt JM, Doubek DL, Krupa TS. J. Am. Chem. Soc 1988;110:2006–2007.
33. Pettit GR, Inoue M, Kamano Y, Dufresne C, Christie N, Niven ML, Herald DL. J. Chem. Soc. Chem. Commun 1988:865–867.
34. Pettit GR, Kamano Y, Dufresne C, Inoue M, Christie N, Schmidt JM, Doubek DL. Can. J. Chem 1989;67:1509–1513.
35. Pettit GR, Xu JP, Williams MD, Christie ND, Doubek DL, Schmidt JM, Boyd MR. J. Nat. Prod 1994;57:52–63. [PubMed: 8158165]
36. Pettit GR, Ichihara Y, Xu JP, Boyd MR, Williams MD. Bioorg. Med. Chem. Lett 1994;4:1507–1512.
37. Pettit GR, Xu JP, Ichihara Y, Williams MD, Boyd MR. Can. J. Chem 1994;72:2260–2267.
38. Pettit GR, Xu JP, Schmidt JM. Bioorg. Med. Chem. Lett 1995;5:2027–2032.
39. Pettit GR, Tan R, Xu JP, Ichihara Y, Williams MD, Boyd MR. J. Nat. Prod 1998;61:955–958. [PubMed: 9677284]
40. D'Auria MV, Giannini C, Zampella A, Minale L, Debitus C, Roussakis C. J. Org. Chem 1998;63:7382–7388. [PubMed: 11672387]
41. Zampella A, Giannini C, Debitus C, Roussakis C, D'Auria MV. Eur. J. Org. Chem 1999:949–953.
42. Giannini C, Zampella A, Debitus C, Menou JL, Roussakis C, D'Auria MV. Tetrahedron 1999;55:13749–13756.
43. Fukuzawa T, Matsunaga S, Fusetani N. J. Org. Chem 1994;59:6164–6166.
44. Fukuzawa T, Matsunaga S, Fusetani N. J. Org. Chem 1995;60:608–614.
45. Fukuzawa T, Matsunaga S, Fusetani N. Tetrahedron 1995;51:6707–6716.
46. Fukuzawa T, Matsunaga S, Fusetani N. J. Org. Chem 1997;62:4484–4491. [PubMed: 11671779]
47. Cheng JP, Lee JS, Sun F, Jares-Erijman EA, Cross S, Rinehart KL. J. Nat. Prod 2007;70:1195–1199. [PubMed: 17580909]
48. Kobayashi M, Kawazoe K, Katori T, Kitagawa I. Chem. Pharm. Bull 1992;40:1773–1778.
49. Morinaka BI, Pawlik JF, Molinski TF. J. Nat. Prod 2009;72:259–264. [PubMed: 19143510]

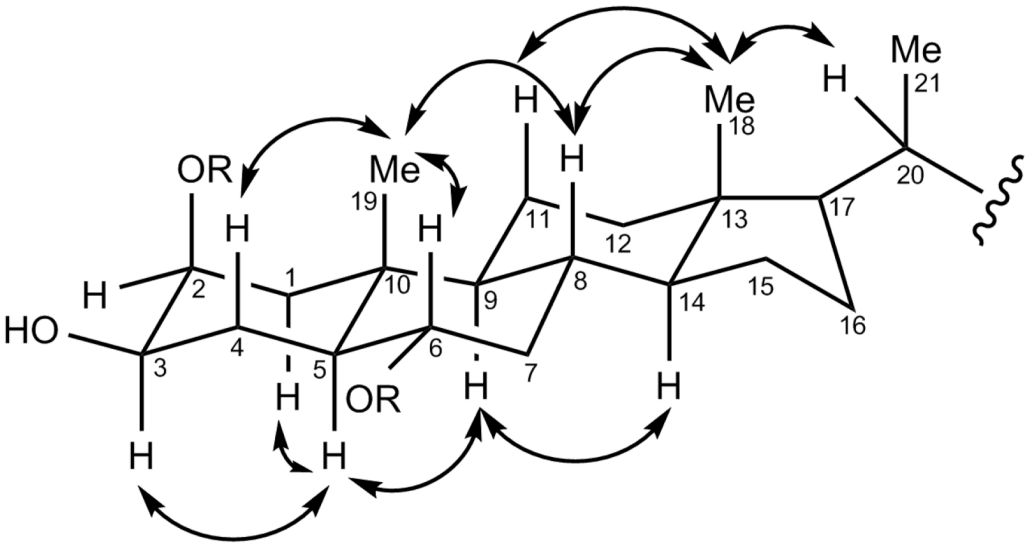

Rings ABCD, R=SO_3Na

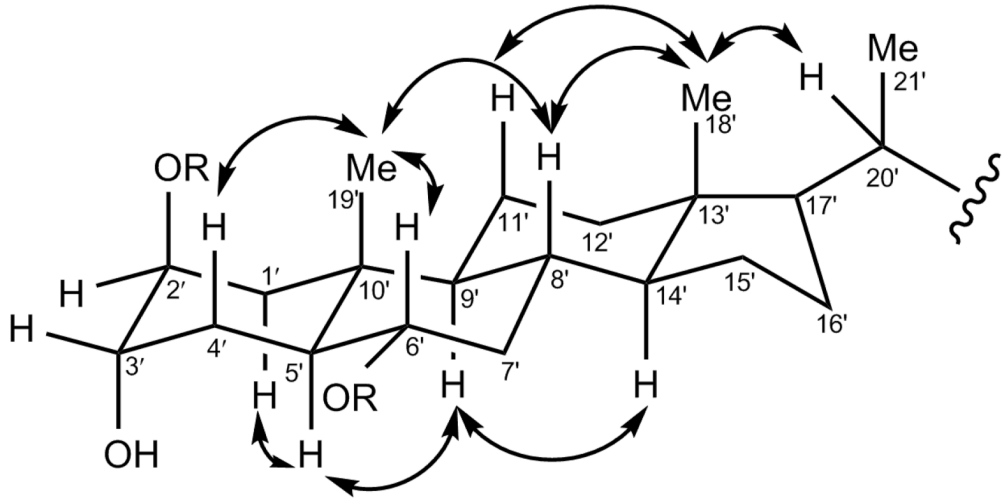

Rings A′B′C′D′, R=SO_3Na

Figure 1.
Key ROE correlations supporting the relative configuration of the ABCD rings, and the A′B′ C′D′ rings of fibrosterol sulfate A (**1**).

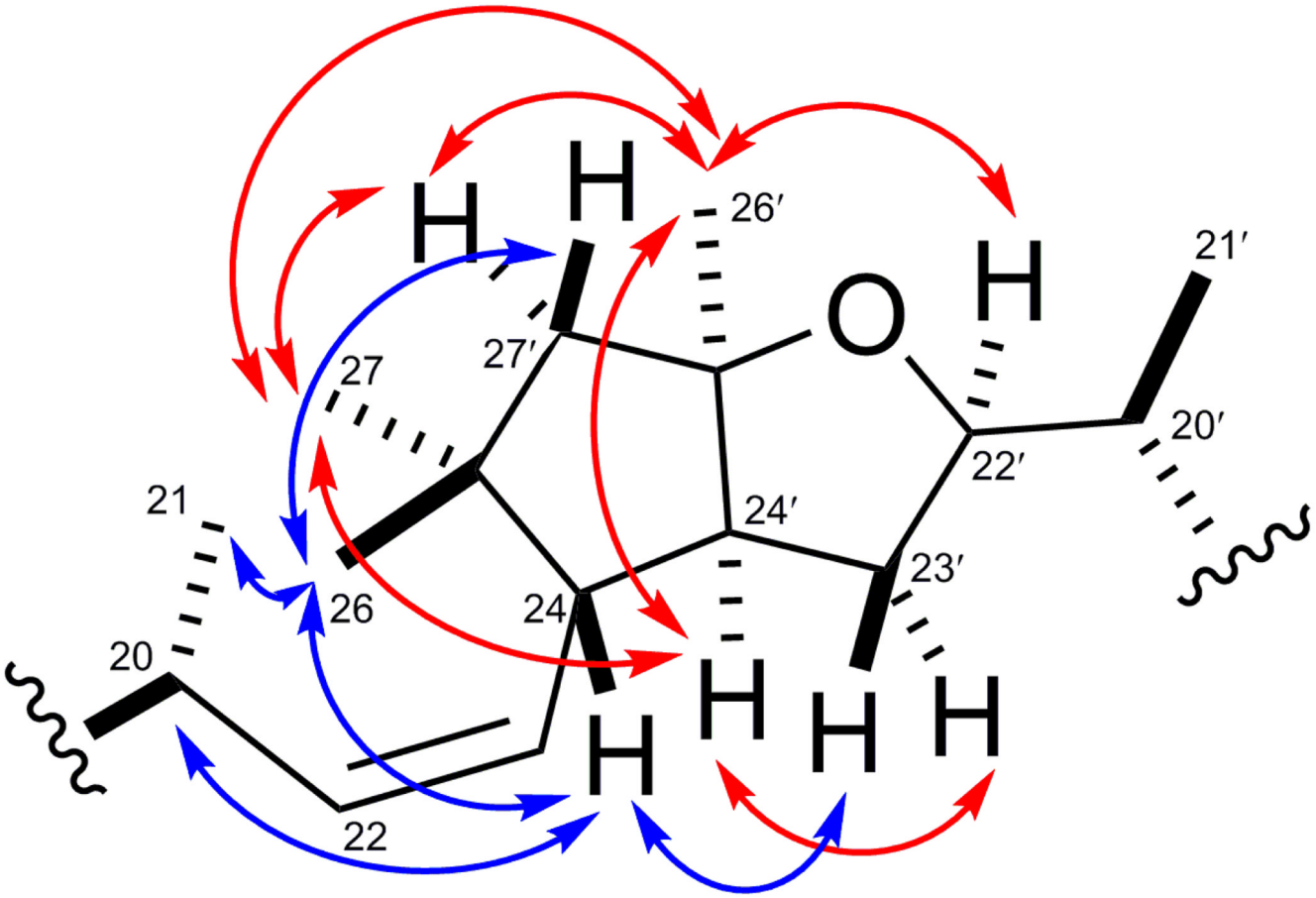

Figure 2.
Key ROE correlations supporting the relative configuration of the bicyclic[3,3,0] octane in the side chain of fibrosterol sulfate C (**3**).

Table 1

NMR data for fibrosterol sulfate A (**1**) (600 MHz, CD_3OD)

position	δ_C	δ_H mult (*J*, Hz)	HMBC	position	δ_C	δ_H mult (*J*, Hz)	HMBC
1α	42.8	1.14,[a] m	5, 9, 10, 19	1α′	38.8	1.47, dd (14.8, 3.5)	9′, 10′, 19′
1β		2.42,[a] m	2, 3, 5, 6, 19	1β′		2.06,[a] m	2′, 3′, 10′, 19′
2	78.2	4.64, m	1, 3, 4, 10	2′	77.8	4.46, m	3′, 4′, 10′
3	72.1	3.58, ddd (11.8, 4.0, 4.0)	2, 4, 5	3′	68.4	4.06, m	1′, 2′, 5′
4α	27.7	2.10, m	2, 3, 5, 6, 10	4α′	26.3	2.04,[a] m	2′, 3′, 5′, 6′
4β		1.62,[a] m	2, 3, 5, 6, 10	4β′		1.72,[a] m	5′, 6′, 10′
5	51.7	1.19,[b] m	1, 3, 4, 6, 7, 9, 10	5′	44.5	1.66,[a] m	1′, 3′, 4′, 6′, 7′, 9′, 10′
6	78.0	4.19,[a] m	4, 5, 10	6′	78.6	4.19,[a] m	4′, 5′, 10′
7α	39.8	0.98,[b] m	5, 6, 8, 9, 14	7α′	39.8	1.06,[b] m	6′, 8′, 14′
7β		2.36,[a] m	5, 6, 8, 9, 14	7β′		2.36,[a] m	5′, 6′, 8′, 9′, 14′
8	35.0	1.53,[a] m	7, 9, 13, 14	8′	35.0	1.53, [a] m	7′, 9′, 13′, 14′
9	55.7	0.69,[b] m	8, 10, 11, 19	9′	55.6	0.75,[b] m	8′, 10′, 11′, 19′
10	37.8	——		10′	38.1	——	
11α	22.1	1.55,[a] m	8, 9, 12, 13	11α′	21.7	1.56,[a] m	8′, 9′, 12′, 13′
11β		1.38, m	9, 10, 12	11β′		1.33,[a] m	9′, 10′, 13′
12α	41.0	1.16,[b] m	9, 11, 13, 18	12α′	41.3	1.18,[b] m	9′, 11′, 13′, 18′
12β		2.01,[a] m	9, 11, 13, 14, 18	12β′		2.02,[a] m	9′, 11′, 13′, 14′, 18′
13	43.9	——		13′	43.8	——	
14	56.9	1.07,[b] m	8, 12, 13, 15, 18	14′	57.4	1.12,[b] m	8′, 13′, 15′, 18′
15α	25.0	1.12,[a] m	13, 14	15α′	25.0	1.12,[b] m	13′, 14′
15β		1.56,[a] m	13, 14	15β′		1.62,[a] m	13′, 14′
16α	28.1	1.30,[a] m	13, 15, 17	16α′	29.1	1.30,[a] m	13′, 15′, 17′
16β		1.74,[a] m	13, 15, 17	16β′		1.87,[a] m	13′, 15′, 17′
17	54.3	1.03,[b] m	13, 16, 20, 21, 22	17′	57.3	1.15,[b] m	13′, 15′, 16′, 18′, 20′, 21′
18	12.4	0.71, s	12, 13, 14, 17	18′	13.1	0.72, s	12′, 13′, 14′, 17′

position	δ_C	δ_H mult (*J*, Hz)	HMBC	position	δ_C	δ_H mult (*J*, Hz)	HMBC
19	15.6	1.08, s	1, 5, 9, 10	19′	15.1	1.05, s	1′, 5′, 9′, 10′
20	43.1	1.69, m (6.6, 3.4)	13, 16, 17, 21, 22, 23	20′	37.7	1.42,[a] m	16′, 17′, 22′
21	12.7	0.97, d (6.6)	17, 20, 22	21′	19.8	0.99, d (6.5)	17′, 20′, 22′
22	76.3	3.98, dd (8.7, 3.4)	17, 20, 21, 23, 24	22a′	36.9	1.69,[a] m	17′, 20′, 21′, 23′, 24′
				22b′		0.99,[b] m	20′, 21′, 23′, 24′
23	126.2	5.35, dd(15.7, 8.7)	20, 22, 24, 25, 27, 24′	23a′	26.6	1.42,[a] m	25, 20′, 22′, 24′, 25′
				23b′		1.07,[b] m	25, 22′, 24′, 25′
24	138.6	5.54, d (15.7)	22, 23, 25, 26, 27, 24′	24′	56.8	1.84,[a] m	
25	47.8	——		25′	157.5	——	
26	24.0	1.15, s	23, 24, 25, 27, 24′	26a′	105.1	4.85[c]	24′, 25′, 27′
				26b′		4.81[c]	24′, 25′, 27′
27a	38.5	1.68,[a] m	24, 25, 26, 24′, 25′, 27′	27′	29.8	2.43,[a] m	27, 25′
27b		1.57,[a] m	24, 25, 26, 24′, 25′, 27′				

[a] Signals overlapped.

[b] Signal buried under overlapping methyl.

[c] Overlapped with HOD signal.

Table 2

NMR data for fibrosterol sulfate B (**2**) (500 MHz, CD_3OD)

position	δ_C	δ_H mult (*J*, Hz)	position	δ_C	δ_H mult (*J*, Hz)
1α	43.0	1.16,[a] m	1α′	39.5	1.47, dd (14.7, 3.5)
1β		2.44,[b] m	1β′		2.06,[b] m
2	78.3	4.67, m	2′	75.4	4.83,[c]
3	72.3	3.59, ddd (11.8, 4.0, 4.0)	3′	75.4	4.76, m
4α	27.9	1.63,[b] m	4α′	24.9	1.80, m
4β		2.12, m	4β′		2.28, m
5	51.7	1.19,[a] m	5′	45.2	1.62, m
6	78.4	4.20,[b] m	6′	78.4	4.20, m
7α	40.0	0.98,[a] m	7α′	40.0	1.05, m
7β		2.37, m	7β′		2.37, m
8	35.0	1.53,[b] m	8′	35.0	1.53, m
9	55.9	0.68,[a] m	9′	55.8	0.74, m
10	38.0	——	10′	37.5	——
11α	22.2	1.38,[b] m	11α′	22.1	1.36, m
11β		1.55,[b] m	11β′		1.55, m
12α	41.1	1.16,[a] m	12α′	41.3	1.19, m
12β		2.02,[b] m	12β′		2.04, m
13	44.0	——	13′	43.9	——
14	57.0	1.08,[a] m	14′	57.3	1.15, m
15α	25.2	1.13,[a] m	15α′	25.1	1.13, m
15β		1.58,[b] m	15β′		1.64, m
16α	28.2	1.31,[b] m	16α′	29.3	1.31, m
16β		1.74,[b] m	16β′		1.88, m
17	54.5	1.05,[a] m	17′	57.5	1.13, m
18	12.7	0.71, s	18′	13.2	0.73, s

position	δ_C	δ_H mult (*J*, Hz)	position	δ_C	δ_H mult (*J*, Hz)
19	15.8	1.08, s	19′	15.2	1.05, s
20	43.1	1.70,[b] m (6.8, 3.4)	20′	37.9	1.42, m
21	13.0	0.98, d (6.8)	21′	19.8	0.99, d (7.0)
22	76.5	3.99 dd (8.7, 3.4)	22a′	36.9	1.71, m
			22b′		0.99, m
23	126.2	5.37 dd (15.7, 8.7)	23a′	26.7	1.43, m
			23b′		1.08, m
24	138.9	5.57 d (15.7)	24′	56.9	1.85, m
25	47.9	——	25′	157.5	——
26	24.2	1.16, s	26a′	105.3	4.87, m
			26b′		4.82,[c] m
27a	38.8	1.68,[b] m	27′	30.0	2.43,[b] m
27b		1.57,[b]			

[a] Signal buried under overlapping methyl signal.

[b] Signals overlapped.

[c] Overlapped with HOD signal.

Table 3

NMR data for fibrosterol sulfate C (**3**) (600 MHz, CD_3OD)

position	δ_C	δ_H mult (*J*, Hz)	position	δ_C	δ_H mult (*J*, Hz)
1α	42.4	1.41,[a] m	1α′	38.8	1.46,[a] m
1β		2.34,[a] m	1β′		2.07,[a]m
2	79.1	4.76, m	2′	77.8	4.42, m
3	71.9	3.71, ddd (11.8, 4.0, 4.0)	3′	68.4	4.08, m
4α	27.9	1.59,[a] m	4α′	26.5	1.76,[a]m
4β		2.08, m	4β′		2.04,[a] m
5	51.0	1.33,[b] m	5′	44.6	1.65,[a] m
6	78.4	4.19,[a] m	6′	78.4	4.19,[a] m
7α	39.9	1.04,[b] m	7α′	39.7	1.04,[b] m
7β		2.38,[a] m	7β′		2.34,[a] m
8	35.0	1.50,[a] m	8′	35.0	1.50,[a] m
9	55.3	0.74,[b] m	9′	55.7	0.75,[b] m
10	37.7	——	10′	37.5	——
11α	21.7	1.33,[a] m	11α′	22.0	1.35,[b] m
11β		1.56,[a] m	11β′		1.58,[a] m
12α	41.0	1.20,[a] m	12α′	41.4	1.13,[a] m
12β		2.01,[a] m	12β′		2.02,[a] m
13	43.4	——	13′	43.9	——
14	57.6	1.14,[a] m	14′	56.9	1.04,[b] m
15α	25.1	1.11,[a] m	15α′	25.1	1.11,[a] m
15β		1.63,[a] m	15β′		1.63,[a] m
16α	29.8	1.29,[b] m	16α′	28.2	1.39,[a] m
16β		1.72,[a] m	16β′		1.76,[a] m
17	57.5	1.22,[a] m	17′	55.2	1.00,[b] m
18	12.9	0.73, s	18′	12.3	0.71, s
19	15.8	1.07, s	19′	15.1	1.05, s
20	35.8	2.45, m (10.8, 6.6)	20′	38.6	1.84,[a] m
21	21.6	1.00, d (6.6)	21′	13.1	1.00, d (6.6)

position	δ_C	δ_H mult (*J*, Hz)	position	δ_C	δ_H mult (*J*, Hz)
22	140.1	5.29 dd (10.8, 10.8)	22′	82.4	4.16,[a] m
23	126.7	5.02 dd (10.8, 10.8)	23*α*′	30.1	1.84,[a] m
			23β′		1.47,[a] m
24	56.6	2.39 m (10.8, 10.1)	24′	56.4	2.24, ddd (10.1, 10.1, 3.3)
25	46.4	——	25′	91.0	——
26	29.3	0.94, s	26′	26.2	1.31, s
27	23.2	0.88, s	27*α*′	56.2	1.66, d (13.9)
			27β′		1.88, d (13.9)